

THE SOLAR SPECTRAL IRRADIANCE FROM 200 TO 2400 nm AS MEASURED BY THE SOLSPEC SPECTROMETER FROM THE ATLAS AND EURECA MISSIONS

G. THUILLIER¹, M. HERSÉ¹, D. LABS², T. FOUJOLS¹, W. PEETERMANS³,
D. GILLOTAY³, P. C. SIMON³ and H. MANDEL²

¹*Service d'Aéronomie du CNRS, F91371 Verrières le Buisson, France,
(e-mail: gerard.thuillier@aerov.jussieu.fr)*

²*Landessternwarte, Königstuhl 12, D69117 Heidelberg, Germany*

³*Institut d'Aéronomie Spatiale de Belgique, 3 avenue Circulaire, B1180 Bruxelles, Belgium*

(Received 28 March 2002; accepted 15 January 2003)

Abstract. The SOLar SPECTrum (SOLSPEC) and the SOLar SPECTrum (SOSP) spectrometers are two twin instruments built to carry out solar spectral irradiance measurements. They are made of three spectrometers dedicated to observations in the ultraviolet, visible and infrared domains. SOLSPEC flew with the ATMospheric Laboratory for Applications and Science (ATLAS) while SOSP flew on the EUropean Retrieval CArrier (EURECA) missions. ATLAS 1 and 2 data being already published, this paper is mostly dedicated to the ATLAS 3 and EURECA data in the IR domain. Comparisons between the ATLAS data sets and the Upper Atmosphere Research Satellite (UARS) results are made. EURECA IR data are shown and compared with previous results. Our best UV, visible and IR spectra are finally merged into a single absolute solar irradiance spectrum covering the 200 to 2400 nm domain.

1. Introduction

The absolute solar spectral irradiance from 200–2400 nm has many interests ranging from solar physics to climatology and Earth's environment physics.

From the ground, observations allow to measure the solar spectral irradiance in the visible and infrared spectral ranges. There are significant absorptions due to several minor constituents of the Earth's atmosphere such as ozone, water vapor, and nitrogen and carbon compounds. The measurements using the method of Bouguer consist in observing at different Sun elevations assuming no absorbent time variations. Non regular concentration of tropospheric constituents raises significant difficulties as encountered typically in the IR domain due to water vapor.

For that particular domain, measurements from aircraft reduce most of the water vapor absorptions. At satellite altitudes, all atmospheric absorptions disappear, but the space environment can affect the instrument performances through optics and electronics degradation.

Existing data in the UV and visible domains have been already reviewed in our previous papers (Thuillier *et al.*, 1997, 1998a, b referred to as Papers 1, 2, and 3, respectively). Below we review the available data in the near IR domain.



TABLE I

Solar spectra with IR data from Arvesen, Griffin, and Pearson (1969), Thekaekara (1974), Burlov-Vassiljev, Gurtovenko, and Matvejev (1995), Colina, Bohlin, and Castelli (1996), Labs and Neckel (1968), and Kurucz and Bell (1995). Range, resolution and increment are given in nm.

Authors	Range	Resolution	Increment
Labs and Neckel (1968)	205–100 000	10 to 100	10 to 100
Arvesen, Griffin, and Pearson (1969)	300–2495	0.1 to 0.3	0.1 to 5
Thekaekara (1974)	120–5000	10 to 100	5 to 100
Neckel and Labs (1984)	329–1247.5	2	1 to 5
Burlov-Vassiljev, Gurtovenko, and Matvejev (1995)	332–1062	1	2 to 5
Colina, Bohlin, and Castelli (1996)	120–2500	1 to 2	1 to 2
Kurucz and Bell (1995)	200–200 000	$\Delta\lambda/\lambda = 500\ 000$	0.01 @300 0.1 @1000 0.3 @2000

Observations in this domain were made by Labs and Neckel (1962). They were obtained from the Jungfraujoch (3570 m altitude) at the center of the solar disk and corrected for center-to-limb variations and atmospheric transmission. They have been revised by these authors who generated a solar spectral irradiance spectrum (Neckel and Labs, 1984). The original data of Labs and Neckel (1962) were used to normalize the solar continuum models of Holweger (1967) and Gingerich and de Jager (1968) allowing to calculate the solar spectral irradiance up to 100 μm (Labs and Neckel, 1968) that we shall use for our comparisons. Arvesen, Griffin, and Pearson (1969) and Thekaekara (1974) carried out observations from airplanes at an altitude of about 12 km. Burlov-Vasiljev, Gurtovenko, and Matvejev (1995) measured from ground the visible and the near IR domains up to 1062 nm. More recently, Colina, Bohlin, and Castelli (1996) have generated a solar spectrum from 120 to 2500 nm by assembling several segments from different origins, namely the UARS data in UV (up to 410 nm), the Neckel and Labs (1984) spectrum (up to 870 nm), Arvesen, Griffin, and Pearson (1969) in the near infrared (up to 960 nm) and a solar model from Kurucz (1993). The IR spectra used in that paper are listed in Table I.

The aim of this paper is to present the final results of our measurements, specially from ATLAS 3, and EURECA missions with a special emphasis on the IR range for the latter, and to present a solar irradiance spectrum from 200 to 2400 nm using our best data. The data from 200 to 870 nm were gathered in March 1992, and are related to a monthly mean of 171 units of the radioflux at 10.7 cm. The IR data from EURECA mission were obtained in September–October 1992, and are related to a radioflux of 132 units. However, given the UV variability, the spectrum

presented below is referred to a solar activity quoted to 171 unit within the solar cycle 22.

2. Instruments, Observations and Data Processing

2.1. INSTRUMENT AND CHARACTERIZATION

2.1.1. *Instrument*

The measurements have been made with the SOLSPEC and SOSP instruments. SOSP is the spare unit of SOLSPEC and the two units have identical design, but different performances, in particular the SOLSPEC instrument has a higher responsivity than SOSP. This has some consequences which will be explained below. Both instruments are composed of three spectrometers named UV, VIS, and IR, made of a double monochromator using holographic gratings. The three spectrometers' optical schematics are similar. The six gratings are mounted on a one-piece mechanical shaft and rotate by using a stepping motor. For the three spectrometers, second-order filters are set on the optical path as a function of the grating step number. The entrance of each spectrometer is made by a quartz diffusor preceding the entrance slit. Internal calibration lamps are included in the instrument: two deuterium lamps are used to monitor the UV, and two tungsten ribbon lamps play the same role for the visible and IR spectrometers. The relationship between the grating step number and wavelength of observation as well as the slit function are characterized by use of an on board helium hollow cathode lamp. The six gratings rotating together, the three wavelength scales are dependent as we have verified experimentally when the instrument was on the ground and later when it was in space.

The detailed designs of the UV and visible spectrometers are given in Papers 1 and 2. The IR spectrometer having a spectral range of 2000 nm, three second-order filters are used as a function of the grating step number. The mean spectral stepping and resolution are 4 and 20 nm, respectively. The latter was chosen especially for the long wavelengths range due to the weak solar spectral irradiance associated with the decrease of the instrument responsivity. The infrared channel detector is a lead sulphide cell from Optoelectronics. Its sensitivity extends from 800 nm to 3300 nm being maximum at 2700 nm. The size of the detector is 2×2 mm and its detectivity is 2.5×10^{11} cm Hz^{1/2} W⁻¹. The detector is enclosed in a TO-8 can including a two-stage Peltier effect thermoelectric cooler which keeps the detector at -15 °C on the ground and in space. The associated electronics is a preamplifier followed by a lock-in amplifier with two gains of 10^4 and 10^5 . The modulation of the signal is made at 512 Hz by a tuning fork from Bulova which gives the reference signal to the lock-in amplifier. The DC signal is sampled by a 12-bit A/D converter. The main IR channel characteristics are given in Table II.

Eleven minutes are required to record the three spectra in UV, visible, and IR domains simultaneously.

TABLE II
SOSP infrared spectrometer characteristics.

IR spectrometer	
Field of view	3.5 arc deg
Spectral range	800–3000 nm
Grating manufacturer	Jobin–Yvon
Diameter	30 mm
Ruled area diam.	17 mm
Ruling frequency	354/mm
Curvature radius	87.4 mm
Focal length	99.42 mm
Bandpass at	1000 nm: 19 nm 3000 nm: 21 nm
Increment per step	4 nm
Entrance window	Infrasil
Surface (mm ²)	0.7 × 10
Detector/type	PbS cell/OTC-22S-8
Detector cooling	$T = -15\text{ }^{\circ}\text{C}$

2.1.2. Characterization

The method and details of the wavelength and instrument responsivity calibration for the UV and visible channels have been given in Papers 1 and 2. The characterization of the IR channel is explained below.

2.1.2.1. *Dispersion Law Measurements.* The purpose of these measurements is to establish the relationship between the wavelength and the grating position number.

To determine the dispersion law of the UV and visible spectrometers, we have employed sources delivering lines of known wavelength. Due to the scarceness of usable lines for the IR spectrometer, we have used a He–Ne laser after withdrawing the second order filters allowing to observe up to order five (3164 nm). These five measurements provided the determination of the wavelength scale. For the UV and visible spectrometers, we used up to 20 lines giving *a priori* a better precision to determine the dispersion law. We have verified the consistency of three spectrometers wavelength scales since the six gratings are rotating together. For these measurements, the gratings rotate by increment of one elementary step (about 0.4 nm). Scanning the slit function allows to define its center to a fraction of a step. This number corresponds to the line wavelength (a multiple of the laser line wavelength) used for that measurement. The dispersion law is found to be parabolic as for the two other spectrometers, and its coefficients are calculated by a

least-squares method. The measurements were carried out in air, but the dispersion law is also valid in vacuum.

These measurements were carried out before and after flight. In orbit, the hollow cathode lamp was activated after each solar observation. This allows to check the UV wavelength scale, and consequently the IR wavelength scale.

2.1.2.2. *Instrument Absolute Responsivity.* The absolute calibration has been performed with the Heidelberg Observatory blackbody. Its cavity made of pure graphite is heated at a temperature which is dependent on the spectrometer to be characterized. The blackbody temperature is read by using a pyrometer calibrated by the Physikalisch-Technische Bundesanstalt (PTB) of Berlin (Germany). The description of the blackbody and the pyrometer are given by Mandel *et al.* (1998).

For the IR domain, the cavity is heated to about 2600 K providing enough signal in the IR domain. This low temperature made the cavity to last several days and allowed to record many spectra without mountings/demountings which could be a source of uncertainties. For calibrating the IR spectrometer, the difficulty is due to the low responsivity in the blue and red wings on the spectrometer and after the filters change. Thirty-two spectra were recorded with the blackbody at 2600 K providing a photon noise smaller than 1%. Measurements of dark current and blackbody temperature were made between each scanning of the IR spectrometer wavelength domain.

For the UV and visible spectrometers calibration, the difficulty remains the blue and red wings of the spectral range of each spectrometer where the responsivity is smaller than in the center of the spectral domain. For the ATLAS instrument (Papers 1 and 2), the instrument responsivity allowed to achieve accurate calibration measurements. However, for the SOSP instrument, we had significant difficulties with each of the spectrometer wings. For reducing the noise, we have performed long exposure times; however, this way has a limit represented by the blackbody stability at the temperature needed by the spectral domain. This is why our calibration coefficients present a larger uncertainty for SOSP than for SOLSPEC in the UV and visible domains. As a consequence, we could not link the three spectrometers' wavelength domains. This is why the corresponding data for SOSP have not been considered in this study, preferring the ATLAS data of better accuracy.

2.2. OBSERVATIONS AND DATA

ATLAS 1-2-3 missions were operated from the Space Shuttle, respectively in March 1992, April 1993 and November 1994, carrying the SOLSPEC spectrometer. As the ATLAS solar payload also carried two other spectrometers observing the UV and the near visible domains, we choose the SOLSPEC instrument for the ATLAS missions for its better performance. During the solar observations, the instrument experienced an unexpected warming increasing with time due to the platform environment. This induced instrumental effects affecting the visible and IR channels.

The increase of the visible detector dark current led to deleting many spectra as already reported. For the IR channel, non-linearity effects at a level of several percent appeared when the signal was high. The data gathered during these missions were only usable in the UV and visible domains (Papers 1, 2, and 3).

The SOLSPEC instrument was turned on during the ATLAS 3 mission starting on 3 November 1993 for a ten-day duration with four periods dedicated to solar observations. A total number of 98 spectra were measured. For the UV domain, 55 were kept spanning all along the mission after selection. However, a wrong command has set the visible spectrometer filter wheel in an erroneous position which led to reject most of the visible spectra. For the six remaining spectra, the data were usable above 420 nm. The ATLAS 3 selected UV and visible spectra were averaged. Each selected spectrum has a dispersion with respect to the mean which is not greater than 2% in UV and 1.1% in visible. These numbers are consistent with the numbers found for the ATLAS 1 and 2 data.

The EURECA mission occurred from 11 August 1992 to May 1993 with the SOSP instrument on board. EURECA is an ESA platform which was placed and retrieved from orbit by the space shuttle. The data from the IR channel of the SOSP instrument are of better quality than on ATLAS for two reasons: (i) the lower responsivity avoided strong signals, and consequently non-linearity effects as observed on ATLAS, (ii) the EURECA platform remained at constant temperature (16 °C) till January 1993. Then the cooling loop was deactivated.

On the other hand, the lower responsivity of the UV and visible SOSP spectrometers led us to prefer using the corresponding data from ATLAS missions.

Since, for the time frame of the EURECA mission, the expected variability in our spectral domain of observations is mainly due to the 27-day rotation, we observed the Sun every two days. Assuming a constant solar spectral irradiance in the IR domain, no aging was encountered (upper limit 0.9%). As the ATLAS 2 mission occurred in April 1993, we also attempted to make correlative measurements with EURECA. Unfortunately, the thermal regulation being deactivated in January, had not allowed operation in appropriate conditions. Before deactivation, SOSP recorded 77 spectra. UV and visible spectra revealed what was expected, a lower signal-to-noise ratio, that is to say noisier data than obtained with ATLAS. These results are not used in the present study as being of less quality than those obtained from the ATLAS missions. However, we observed the solar variability using the Mg II line and we derived the Mg II index similarly to DeLand and Cebula (1998).

2.3. DATA PROCESSING

2.3.1. *Processing of the Calibration Measurements*

The blackbody temperature was measured at the beginning and at the end of each run, allowing to reject measurements when the temperature was changing by more than 5 K. Using Planck's law, the measurements were normalized at a temperature equal to the mean blackbody temperature corresponding to the run. These normal-

ized spectra were averaged, and after calculating the blackbody spectral irradiance, the calibration coefficients were derived. This procedure is similar to one used in the UV and visible spectrometers calibration, and is detailed in Papers 1 and 2.

2.3.2. *Processing of the Solar Measurements*

The UV and visible SOLSPEC-ATLAS 3 data which will be shown in the next section, were selected according to the criteria given in Papers 1 and 2. In particular, the on-board hollow cathode lamp allows to check the wavelength scale stability as well as the Mg II Fraunhofer line at 280 nm.

EURECA IR spectra are selected using the following criteria :

- no partial absorption by the Earth's atmosphere, which occurs when the line of sight (instrument to Sun) has a tangent height smaller than 100 km,
- complete spectrum,
- wavelength scale stability,
- platform pointing stability.

The wavelength scale stability is an important criterion. As we have no direct check of the IR wavelength scale, we have used the Mg II Fraunhofer line profile measured at the same time by the UV spectrometer. When shifted Mg II line profiles were measured, the corresponding IR spectra were rejected.

Another important criterion is the Sun position within the instrument field of view. The IR entrance slit (0.7×10 mm) is significantly greater than the visible one (0.15×1 mm). It results a dependence of the instrument responsivity when a source such as the Sun is moving in the field of view. In orbit, the Sun position was measured by the solar sensor of the DIARAD radiometer (Crommelynck *et al.*, 1993). As the SOSP and the DIARAD instruments optical axis have not been precisely related, the Sun sensor indicated a Sun position variation rather than an absolute position. A dependence was found between the SOSP signal and the DIARAD depointing signal when the latter was greater than 0.75 arc deg. The r.m.s. dispersion for a depointing angle smaller than 0.75 arc deg was 1.7%, but increased above 2.5% for this angle reaching 2 arc deg. After applying this criterion (0.75 arc deg), sixteen spectra remained corresponding to the two first months of the mission. The Sun position in the field of view was the most selecting criterion.

In order to increase the measurement range, the IR channel electronics has two outputs, IR1 (low sensitivity) and IR2 (high sensitivity), having a ratio set to 9.9. We use the data from one or other channel according to the level of signal in order to avoid non linearity and to have the best signal-to-noise ratio. Given the solar spectral irradiance and the instrument responsivity decrease as a function of wavelength, the most sensitive output is used above 1800 nm.

Afterward, the raw data have been normalized to one astronomical unit. These remaining spectra were averaged, and the ratio of each spectrum to the mean was calculated. These ratios remain around unity within $\pm 1\%$.

2.3.3. *Uncertainty Analysis*

The uncertainty analysis of the UV and visible data obtained during the ATLAS 3 mission has been carried out as for the ATLAS 1 and 2 missions (Papers 1 and 3) with similar results. However, the IR data uncertainty analysis is new and is shown below.

2.3.3.1. *Uncertainty in the Absolute Calibration (Table IIIb)*

(a) From the pyrometer calibration:

the calibration of the pyrometer was made by the PTB which also provides the corresponding uncertainty affecting the transfer of the PTB scale to our measurements. This allows to estimate the systematic uncertainty due to the scale transfer affecting the blackbody irradiance which is found to decrease with increasing wavelength from 0.9 to 0.4% in the IR domain.

(b) From the blackbody temperature reading:

the blackbody temperature is obtained from the pyrometer output. For a constant temperature, the statistical fluctuation of the reading is 20 mV. This corresponds to 4 K for a blackbody temperature of 2600 K as encountered during our measurements. Using the Planck's law, we derive the corresponding 2σ statistical uncertainty and find 1.8% at 950 nm and 0.8% at 2500 nm.

(c) From the wavelength scale:

the spectrometer has to be set at a well-defined wavelength during the calibration and the solar measurements. As no line is available in the IR domain, and the IR and UV spectrometers being mounted on the same mechanical shaft, the 2σ uncertainty in UV was transferred in 2σ uncertainty in the IR domain. It is found to be 0.25 nm. For a 2600 K blackbody temperature, this figure generates a statistical uncertainty varying from 0.06% at 950 nm and 0.045% at 2500 nm.

(d) From the distance between the blackbody and the instrument:

this distance is adjusted by the use of a metallic rod. It is checked before and after each calibration run with an accuracy of 0.1 mm for a total distance of 850 mm. This systematic uncertainty is negligible (0.04%).

(e) From the blackbody aperture:

its surface is 49.901 mm². Its accuracy is quoted by the manufacturer to be 0.2%. As the brass aperture is cooled to 20 °C, there is no correction for thermal expansion. This systematic uncertainty will be taken into account in the accuracy budget.

The diffraction effect is negligible as the aperture diameter is 3000 times the maximum detectable wavelength of the IR spectrometer.

(f) From the misalignment:

the optical instruments generally present a responsivity slightly dependent of the source position in the field of view. As a diffusor is used, the angular response should be constant, and sharply decreasing on the edges due to vignetting. Actually, the center field of view is not a plateau, and we measured 1% per arc deg deviation from the optical axis. This is why the instrument and the blackbody optical axis

should be co-aligned. An autocollimation was made by reflecting a laser beam through the blackbody cavity mounting on the spectrometer preslit. The resulting uncertainty is less than 15 arc min. Since the blackbody aperture is seen from the instrument preslit (first optical surface of the spectrometer) under a solid angle close to that of the Sun, we estimated the systematic uncertainty induced by the misalignment during calibration to 0.25%.

(g) From the air transmission:

during the blackbody calibration, the instrument is flushed with dry nitrogen. However, the optical path length of 85 cm between the blackbody and the entrance diffusor is in air. But, this distance is too short to give a noticeable absorption in the IR range except around 1.35 μm and 1.9 μm where it could reach 0.1% due to H₂O absorption bands.

(h) From the dark current and electronics stability:

the PbS cell as for many infrared detectors is not photon-noise limited. This means that the uncertainty due to this detector is dominated by the fluctuation of its dark current and that the photon noise is negligible with respect to the latter. Its mean value for the less sensitive output of the IR electronics is 15 relative units with a standard deviation of 5 for the selected spectra. This includes the noise from the intrinsic detector dark current, the pre-amplifier, and the lock-in amplifier electronics.

To estimate the stability of the IR detector and its associated electronics, we have used a NIST tungsten lamp and found a standard deviation of 0.15%. This figure represents the IR channel stability since the FEL lamp DC current is stable to 10^{-4} . Furthermore, this is an upper limit because the thermal environment of the lamp may be not strictly stable.

(i) From the instrumental slit function:

each measurement results in the convolution of the source spectrum by the instrumental slit function. The calibration coefficient being determined by observing the blackbody, an uncertainty is generated because of the different gradients of the Sun and blackbody spectral distributions. For the case of the IR solar continuum, the uncertainty is smaller than 0.01%. Greater uncertainties could be generated in presence of deep Fraunhofer lines which is not the case of the IR part of the solar spectrum.

(j) From the responsivity within the field of view:

as explained previously, the responsivity decreases from the center to the edge of the field of view. The blackbody being a uniform source, and the Sun surface presenting a limb-darkening, this results in a systematic uncertainty which has been estimated as follows: first, we integrate the solar radiance in the field of view taking into account the variation of responsivity, and second we operate similarly with the blackbody. Making the difference, we obtained an overestimate of 0.16% of the solar irradiance at 1500 nm. The responsivity variation in the field of view was also measured at some other wavelengths in the IR spectrometer domain. Given the presence of the noise, no significant variation with wavelength was found.

2.3.3.2. *Uncertainties during the Solar Observations (Table IIIc)*

(a) From the wavelength change:

the wavelength scale is checked in flight by using the hollow cathode lamp in the UV channel. As explained above, the uncertainty of the IR channel wavelength scale is 0.25 nm resulting in a statistical uncertainty of 0.14% at 950 nm and 0.05% at 2500 nm taking into account the 20 nm width IR slit function.

(b) From the dark current and electronics fluctuations:

we have seen (2.3.3.1.(h)) that for calibration measurements a 2σ uncertainty of 0.3% can be estimated as resulting of the sum of the dark current and IR channel electronics noise.

In flight from the housekeeping parameters, it is verified that the detector temperature is maintained at the same value as during ground calibration, and that the dark current is the same as at ground. The IR electronics have built-in temperature correction, and as the electronics during flight kept a temperature close to the one on the ground, we estimate that the amplification factor is the same in orbit and on the ground. Furthermore, the signal from the Sun being greater than the one from the blackbody, we can keep 0.3% (2σ) as an upper limit for the statistical uncertainty resulting of the dark current and IR channel electronics.

(c) From the pointing:

given the size of the IR slit, the responsivity is slightly variable in the field of view as we measured in the laboratory. Due to the variable pointing, it results in an uncertainty affecting each spectrum. However, we did not correct the selected spectra owing to a lack of precise information about alignment between SOLSPEC and DIARAD. We only know that the mechanical alignment was likely better than 10 arc min. Consequently, we decided not to take into account the pointing for each spectrum, and we only calculated the mean of the selected spectra. As depointing was close to be random, we estimated the resulting 2σ statistical uncertainty at 0.5%

2.3.3.3. *Total Uncertainty*

All uncertainties (a)–(c) contribute to making a spectrum slightly different from any other one. Uncertainties are either random or systematic. The former can be added geometrically. As we ignore the sign of the latter, they will be combined by the same way.

Consequently, the resulting 2σ uncertainty is calculated as a function of wavelength and is given in Table III as subtotal (2). The measured variance of the selected spectra is given in Table IIIa. We note that the calculated 1σ variance is in general smaller than the measured one which suggests some unknown source of uncertainties. At 2500 nm, there is a significant increase of the measured variance (top of Table III) indicating that the limit of the reliability of our measurements is reached.

TABLE III

SOLSPEC identified sources of uncertainties and their estimates (%) as a function of wavelength. (a) gives the variance of the selected spectra. (b) and (c) provide the uncertainty budget for measurements carried out in calibration and in orbit respectively.

(a) Variance of the selected spectra				
Wavelength (nm)	950	1500	2000	2500
Variance (%)	1	1	1	3
(b) Sources of uncertainty in calibration (2σ)				
(a) Pyrometer calibration	0.9	0.6	0.5	0.4
(b) Pyrometer reading	1.8	1.2	0.9	0.8
(c) Wavelength scale	0.06	0.06	0.05	0.04
(d) Distance	0.04	0.04	0.04	0.04
(e) Aperture	0.2	0.2	0.2	0.2
(f) Misalignment	0.5	0.5	0.5	0.5
(h) Photon noise and IR electronics stability	0.3	0.3	0.3	0.3
(j) Responsivity in the field of view	0.16	0.16	0.16	0.16
Sub-total (1)	2.1	1.	1.2	1.1
(c) Sources of uncertainty in solar measurements (2σ)				
(a) Wavelength shift	0.14	0.1	0.08	0.05
(b) Photon noise and IR electronics stability	0.3	0.3	0.3	0.3
(c) Pointing	0.5	0.5	0.5	0.5
Sub-total (2)	0.6	0.6	0.6	0.6
Total (1) + (2)	2.2	1.6	1.3	1.2

3. Results and Comparisons

3.1. SOLSPEC RESULTS

3.1.1. UV Domain Observed during the ATLAS 3 Mission

To compare the data obtained during the ATLAS 3 mission with ATLAS 1, we follow the method as used previously (Cebula *et al.*, 1996): (i) The ratio of the two spectra is calculated using a 5 nm running mean; the mean ratio with respect to unity provides the percentage of difference. (ii) The RMS of the fluctuation of the ratio of the two spectra around its mean, is deduced. This method will be applied in this article to perform comparisons.

TABLE IV

Comparison of results obtained by SOLSPEC with SSBUV and SUSIM on board ATLAS 3, with the mean UARS ATLAS 1 and 2 spectra, and with SOLSTICE and SUSIM on board UARS. The mean difference with respect to unity is given in percentage. The standard deviation for the comparisons made in this table are all around 2%. ATL stands for ATLAS.

Ratios	< 230	230–320	320–350	200–350
A SOLSPEC1/SOLSPEC 3	4.7	–1.2	–0.4	0.1
T SSBUV3/SOLSPEC 3	1.0	0.1	–3.1	–0.4
L SUSIM3/SOLSPEC 3	–3.8	–1.5	–4.2	–2.5
UARS/SOLSPEC 1	–1.7	2.0	–2.3	0.4
UARS/SOLSPEC 2	0.2	0.9	–1.3	0.3
U SUSIM/SOLSPEC1	–0.8	3.1	–3.2	1.0
A SOLSTICE/SOLSPEC1	1.0	3.2	–2.4	1.5
R SUSIM/SOLSPEC2	–6.6	–3.8	–4.2	–4.4
S SOLSTICE/SOLSPEC2	4.1	2.9	–0.6	2.4
SUSIM/SOLSPEC3	–2.1	–1.2	–3.7	–1.9
SOLSTICE/SOLSPEC3	4.6	2.6	–2.5	1.9

Table IV compares the UV SOLSPEC ATLAS 1 to ATLAS 3. These two spectra agree for the mean within 1.5% and within 3% for the r.m.s. deviation of all observations above 230 nm (first line of Table IV). Below 230 nm, the solar irradiance observed during the ATLAS 3 mission is smaller than during the ATLAS 1 mission as an expected effect of the decreasing solar activity.

3.1.2. Visible Domain Observed during the ATLAS 3 Mission

The visible spectrum recorded during the ATLAS 3 mission is compared to ATLAS 1 in Table V in three spectral intervals. The measurements show consistent results in terms of r.m.s. difference of all observations around 1.5%, a mean difference not greater than 0.5%, and a mean of 0.4% for the 420–800 nm domain (Table V).

3.1.3. Infrared Domain Observed during the SOSP-EURECA Mission

The spectrum as a function of wavelength is expected to be very smooth due to the bandpass close to 20 nm and due to the absence of large equivalent width Fraunhofer lines. This result is supported by making the integration of the spectrum of Kurucz and Bell (1995) within the SOSP slit function, which, however, shows some slight residual Fraunhofer signatures at the level of a few percent.

After selecting the raw data according to the criteria explained in 2.3.1, and applying the calibration coefficients, the SOSP solar spectral solar irradiance was

TABLE V

Comparisons between the ATLAS 1 and 3 SOLSPEC visible spectra for three wavelength domains. The mean difference with respect to unity is given in percentage. For the comparison in the visible range of ATLAS 3 results, the domain is limited to 420 nm for the shortward wavelength. The standard deviation for the comparisons made in this table are all below 1.5%.

Ratio	420–450	450–800	420–800
SOLSPEC1/SOLSPEC3	−0.5	0.4	0.4

obtained. Variations of 1 to 2% amplitude were noticeable with respect to the mean due to possible instrument noise, nearby second-order filters change, and minor Fraunhofer lines contribution given the 20 nm resolution. To smooth these variations, we have performed a least-squares method with a parabola linking the last point of the visible spectrum (876.86 nm) to 959.9 nm and a 6-deg polynomial above, but keeping the same derivative at that wavelength. Due to the measured variance increase at 2500 nm (top of Table III), we have limited our IR observed domain to 2400 nm.

3.2. COMPARISONS WITH OTHER DATA SETS

3.2.1. *In the UV Domain*

Other UV spectral irradiance observations were obtained from the ATLAS and UARS missions. On board the three ATLAS missions were placed two other grating spectrometers the Solar Ultraviolet Spectral Irradiance Monitor (SUSIM) (Woods *et al.*, 1996; VanHoosier, 1996; Floyd *et al.*, 2002), and the Shuttle Solar Backscatter UltraViolet (SSBUV) instrument (Cebula *et al.*, 1996; Cebula, Huang, and Hilsenrath, 1998). Comparisons of these data sets were already reported for ATLAS 1 and 2 (Papers 1, 2, 3).

The SSBUV measurements at the same time agree within 2% (r.m.s.) and 1 to 2% for the mean except above 320 nm where the difference reaches 3%. However, for the range 200–350 nm, the agreement stays below 1%. The SUSIM spectrometer also observing at the same time does not show a similar agreement, in particular below 230 nm. Again, the agreement improves when the range 200–350 nm is considered. Above 320 nm, SOLSPEC irradiance is greater than SUSIM and SSUBV by 3 to 4%. The r.m.s. of the differences between the three instruments for the three flights always remain of the order of 2%.

Figure 1 shows the ratio of the SSBUV (Cebula *et al.*, 1998), SUSIM (Floyd *et al.*, 2002) to SOLSPEC for ATLAS 3 mission using the method of the running mean at 5 nm resolution. Similar comparisons were already shown for the two first missions. The presence of deep Fraunhofer lines generates oscillations of

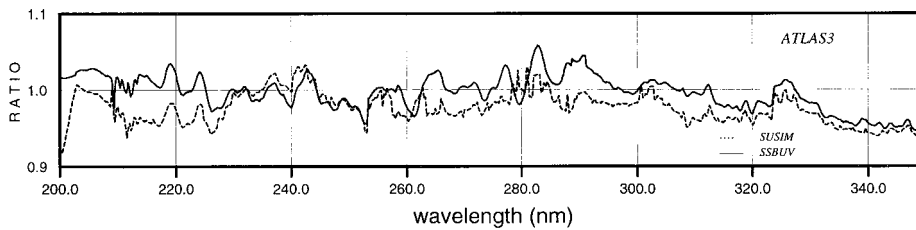


Figure 1. Running mean at 5 nm resolution ratio of the SSBUV and SUSIM to SOLSPEC spectra measured during the ATLAS 3 mission.

the ratio as for example around the Mg II line at 280 nm (Figure 1). The agreement/disagreement is a function of the wavelength domain (e.g., 200–250 nm) and depending on the instrument. For example, the discrepancy with respect to SUSIM between 260 and 280 nm is not found with SSBUV. Below 230 nm these two data sets have opposite behaviour. As shown for ATLAS 1 and 2, the best agreement is found with SSBUV. However, we note that this agreement degrades down to 4% above 330 nm for both SUSIM and SSBUV results as shown in Table IV.

On board UARS, two spectrometers were placed, the SOLar STellar Irradiance Comparison Experiment (SOLSTICE) (Rottman, Woods, and Sparn, 1993), and SUSIM (Brueckner *et al.*, 1993), identical to the one run on board ATLAS. They were in operation during the ATLAS missions. Two mean spectra corresponding to the ATLAS 1 and 2 missions were built (Woods *et al.*, 1996) which are in a better agreement with SOLSPEC above 320 nm than SOLSPEC with respect to SSBUV and SUSIM. For the range 200–350 nm, the mean UARS spectra, SSBUV and SOLSPEC are the three spectra having the closest agreement (Table IV). Table IV also shows comparison of SOLSPEC with the UARS instruments. The r.m.s. differences are generally higher than with ATLAS instruments, reaching about 4% as well as for the mean over the 200–350 nm range. Furthermore, SUSIM may behave differently with respect to SOLSTICE depending on the ATLAS period. This is illustrated by Figure 2. SOLSTICE and SUSIM agree for the full spectral range for ATLAS 1, while SOLSPEC shows its best agreement only below 240 nm. For ATLAS 2 a different situation is found: SUSIM and SOLSTICE disagree mainly below 300 nm in opposite directions, while SOLSPEC appears as their mean value. Below 300 nm for ATLAS 3, similar features as for ATLAS 2 are found, but with smaller differences. This shows that the instrumental uncertainties are not evenly distributed and that the use of mean spectra, e.g., the mean ATLAS 1 versus the mean UARS, shows the best agreement (Cebula *et al.*, 1996).

3.2.2. In the Visible Domain

Comparisons with other spectra either obtained from high-altitude observatories or planes have been shown in Papers 2 and 3. Due to the small difference between ATLAS 3 and ATLAS 1, these comparisons are not repeated. However, for the observed domain 420–450 nm, the difference with the spectrum of Neckel and

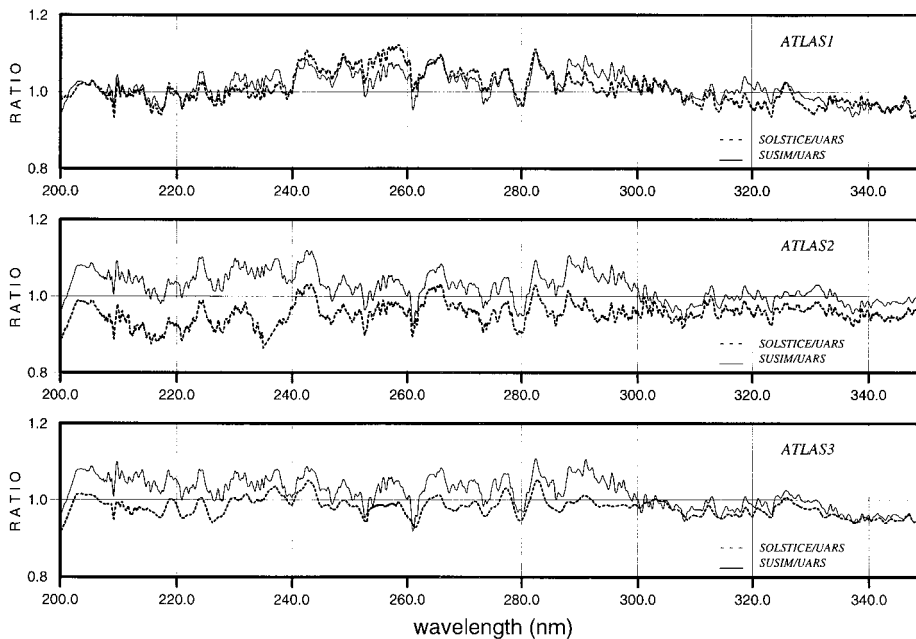


Figure 2. Running mean at 5 nm resolution ratio of the UARS SOLSTICE and SUSIM to SOLSPEC spectra measured during the three ATLAS missions.

Labs (1984) is confirmed. Furthermore, the synthetic spectrum of Kurucz and Bell (1995) agrees within 2% from 350 to 850 nm with SOLSPEC ATLAS 1, and below 400 nm, it is also closer to SOLSPEC than to the spectrum of Neckel and Labs (1984).

3.2.3. In the IR Domain

Figure 3 shows ratios of the SOSP IR solar irradiance to several infrared spectra at 20 nm resolution using a running mean. The spectrum of Arvesen *et al.* (1969) shows an agreement with SOSP quoted to 0.4% for the mean between 1000 and 1700 nm (Table VI) which degrades above. The most important discrepancies are observed around 1700, 1900 and above 2000 nm (Figure 3). Indeed, the high-resolution spectrum from Livingston and Wallace (1991) recorded from the ground up to 5000 nm, clearly shows absorptions features at these wavelengths. In addition, SOSP being retrieved after the mission, measured from the ground the solar spectral irradiance which showed the above features. These discrepancies are due to an atmospheric absorption by water vapor, methane and carbon dioxide insufficiently corrected. Thekaekara (1974) presents its major discrepancy above 1700 nm and appears the least reliable when compared to all other spectra (Table VI).

The IR part of the spectra from Labs and Neckel (1968), Colina *et al.* (1996), and Kurucz and Bell (1995) behave very closely, likely per construction. They show a trend reaching 5% at 1900 nm which decreases above and reaches 2% at

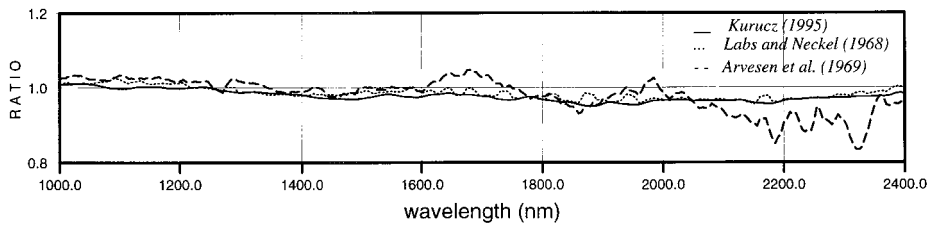


Figure 3. Running mean ratio at 20 nm resolution of several IR spectra to SOSP from 1000 to 2400 nm after normalization of the latter by 1.4%.

TABLE VI

Comparisons between the SOSP infrared spectrum with ground and plane measurements in two wavelength domains (900–1700 nm and 1700–2000 nm). The mean value (m) with respect to unity, and standard deviation (σ) are given in percentage.

SOSP-EURECA compared to	900–1700		1700–2000	
	m	σ	m	σ
Labs and Neckel (1968)	–1.4	0.9	–4.2	0.7
Arvesen, Griffin, and Pearson (1969)	–0.4	1.6	–3.1	2.9
Thekaekara (1972)	–1.5	3.0	–11.0	4.1
Colina, Bohlin, and Castelkli (1996)	–2.8	1.3	–5.7	1.8
Kurucz and Bell (1995)	–2.0	1.2	–5.1	1.8

2400 nm (Figure 3 and Table VI). This indicates a solar irradiance as measured by SOSP greater than the spectral irradiance given by these spectra. As for the Neckel and Labs (1984) data, they remain greater than Burlov-Vasiljev, Gurtovenko, and Matvejev (1995) and SOSP from 900 to 1250 nm by about 3%. Fox, Fontenla, and White (2002) recently have generated a solar irradiance spectral synthetic model obtained by radiative transfer calculations taking into account the distribution of the various magnetic structures in the solar atmosphere and incorporating, to various degrees, all known continua, atomic and molecular opacity sources, populations and ionization stages (Avrett, 1998; Fontenla *et al.*, 2001; Fox, 2003). The difference between this spectrum and SOSP is much smaller than the difference between SOSP and the spectrum of Kurucz and Bell (1995).

4. The Spectrum from 200 to 2400 nm

As explained previously, the data sets in UV and visible from the EURECA mission are of lesser quality than those from ATLAS missions, while the ATLAS IR data are not reliable. Consequently, to build a spectrum from 200 to 2400 nm, we have

used our best measurements, i.e., the UV and visible ATLAS 1 data, and the SOSP IR measurements obtained four months later. This is allowed by the negligible variability in this wavelength range, given the time interval (Fontenla *et al.*, 1999).

We have published our UV and visible results (Papers 1, 2, and 3). Paper 3 is a revision of the visible spectrum between 820 and 870 nm by choosing measurements recorded in the coolest conditions of observations as explained in the references above.

For an unknown reason, an absence of calibration data was noted between 670 and 688 nm, inducing a corresponding gap in our observations of the solar spectral irradiance. As at these two wavelengths, the SOLSPEC and Neckel and Labs (1984) data being in agreement within 1%, we have used their data rather than making an interpolation. A merging of UV and visible spectra was made around 350 nm to ensure continuity.

The resulting spectrum from 200 to 2400 nm has a resolution of about 1 nm below 870 nm and 20 nm above for the IR spectrometer. A spectrum having two significant different resolutions is not convenient for atmospheric studies which generally require a resolution close to 1 nm in the whole range. Therefore, we have considered to scale a high-resolution spectrum on our IR data. We choose the spectrum of Kurucz and Bell (1995) because it covers the spectral range above 2400 nm which will be useful as will be shown below. For doing that, we have to integrate the spectrum of Kurucz and Bell (1995): integrating in the instrument slit function (20 nm) produced a significant smoothing, but still leaves the signature of the Fraunhofer lines presence in this domain. Consequently, we have integrated the spectrum of Kurucz and Bell (1995) at 50 nm resolution to generate a spectrum as smooth as the SOSP one in its polynomial form. The ratio of these two spectra allowed to make the scaling. For consistency in terms of resolution with the UV and visible data, the high-resolution spectrum of Kurucz and Bell (1995) has been degraded to 1 nm and then scaled to SOSP data. These calculations were verified by integration of the resulting spectrum over 50 nm and compared to the polynomial representation of the SOSP data (Section 3.1.1).

Furthermore, several solar spectra already published have been normalized on a given value of the total solar irradiance (TSI) (e.g., World Radiation Center spectral irradiance model (WRC), Wehrli, 1985; Colina, Bohlin, and Castelli, 1996; Kurucz and Bell, 1995; Labs and Neckel, 1968). The TSI could be derived from our measurements if energy below 200 nm and above 2400 nm are estimated.

To estimate the energy below 200 nm, we first use the EUV spectral distribution and its variability based on rocket measurements (Woods *et al.*, 1998) made in the 1992–1994 time frame, i.e., covering the ATLAS period. Secondly, to cover the spectral interval between Lyman α to 200 nm, we use the mean UARS spectrum (Woods *et al.*, 1996) corresponding to ATLAS 1. Finally, we found that the energy below 200 nm was 0.11 W m^{-2} . However, this estimate cannot significantly change the energy budget that we are making.

TABLE VII

Solar spectral irradiance at 2400 nm and energy above given by the spectra of Labs and Neckel (1968) and Kurucz and Bell (1995). LN (1968) and KB (1995) stand for these two spectra, respectively. The spectral irradiance is given in $\text{mW m}^{-2}\text{nm}^{-1}$, and the energy in W m^{-2} .

	LN (1968)	KB (1995)	SOSP
Spectral irradiance	60.43	59.90	61.30
Energy above	52.22	51.45	

To estimate the energy above 2400 nm, we use either the spectra of Kurucz and Bell (1995) or Labs and Neckel (1968) because both allow integration up to 100 μm . These models provide the spectral irradiance at 2400 nm and the energy above. The results are shown in Table VII. Consequently, taking the complement above 2400 nm from Kurucz and Bell (1995), the total solar irradiance (TSI) is obtained by summing: $0.11 + 1334.1 + 51.45 \times 61.3 / 59.9 = 1386.86 \text{ W m}^{-2}$. Now, taking the complement from Labs and Neckel (1968), we find 1387.29 W m^{-2} . These two determinations are very close.

Crommelynck *et al.* (1996) measured the TSI at the same time during the ATLAS 1 mission using the SOLCON/DIARAD radiometer and found 1365.13 W m^{-2} with an accuracy of 0.1%. Comparisons of TSI measured by two or three instruments at the same time show slight discrepancies which led Fröhlich and Lean (1998) to produce a mean composite TSI model which provides 1367.7 W m^{-2} at the time of our measurements. The difference between the radiometric TSI determination and ours, is around 20 W m^{-2} , which is mainly originating from above 350 nm. Comparing our reconstructed TSI with these two determinations shows a difference of 1.6% using SOLCON/DIARAD results and 1.4% using the mean composite TSI model. Furthermore, the complement estimated from the models of Kurucz and Bell (1995) or Labs and Neckel (1968) does not change these results significantly. As the TSI given by Fröhlich and Lean (1998) is very close to the TSI corresponding to the spectrum of Kurucz and Bell (1995) (quoted to 1368 W m^{-2}), we shall adopt 1.4% as percentage of normalization. This normalization is justified by the accuracy of the radiometric instruments (0.1%) being higher than the spectrometers accuracy which is about 2% at best. We note that the normalization percentage is within the quoted accuracy of the spectral data. The 1.4% difference appears as a systematic uncertainty. We have shown that a source of systematic uncertainty is the pyrometer calibration (Papers 1 and 2). A difference of 20 W m^{-2} cannot be attributed in the UV domain (see for example Table VIII), but more likely to the visible domain and the IR domain, but to a lesser extent. We made this estimate in Paper 3, and found 1.1% at 500 nm. Other uncertainties also contribute,

TABLE VIII

Energy in several wavelength domains given by the spectra covering the 200–2400 nm domain. Columns 1 to 4 are expressed in percentage of the energy of the 200–2400 nm interval. In percentage, the two last lines are identical. The last line (*) includes the 1.4% reduction and provides the energy per wavelength interval. Energy is given in W m^{-2} . ** indicates the TSI calculated by integration of the SOLSPEC and SOSP data complemented above 2400 nm by the spectrum of Kurucz and Bell (1995).

Spectral domain (μm)	0.2–0.35	0.35–0.5	0.35–1	1–2	0.2–2.4	TSI
Labs and Neckel (1968)	4.1	18.2	68.2	24.9	1313.8	1366
Colina, Bohlin, and Castelli (1996)	4.3	18.4	68.3	25.2	1311.3	
WRC	4.1	18.2	67.8	25.6	1316.1	1367
Kurucz and Bell (1995)	4.4	18.4	68.1	25	1316.5	1368
SOLSPEC	4.2	18.6	67.8	25.3	1334.1	1386.8**
SOLSPEC*	55.8*	244.8*	892.5*	332.8*	1315.7*	1367.7

in particular the pyrometer reading and photon noise during calibration. But, very likely the systematic uncertainty affecting the pyrometer calibration is the main source of the 1.4% difference found in this study, and the PTB scale cannot be considered as the source of this bias.

Applying the 1.4% normalization percentage, the resulting spectrum allows several comparisons per wavelength interval for different spectra as shown in Table VIII. We only used spectra covering the complete 200–2400 nm range. For each interval, we calculated the energy and the corresponding percentage with respect to the energy of the 200–2400 nm interval. This allows us to examine how the energy is distributed within the different spectra. All percentages are close and the differences are smaller than the systematic uncertainty affecting the spectra used in this comparison. We also note that in the 200–350 nm interval, the solar variability should be taken into account as these spectra are not obtained at the same time. However, in the 350–500 nm interval, all percentages indicate more energy than given by the spectra of Labs and Neckel (1968) and WRC, as expected from the direct comparison of the concerned spectral irradiance (Papers 2 and 3). This is compensated in the 500–1000 nm range where SOLSPEC and WRC agree. In the range 1000–2000 nm, the best agreement is found with Colina, Bohlin, and Castelli (1996). We also note that the difference between SOLSPEC and the spectrum of Kurucz and Bell (1995) remains of the order of 0.2–0.3%. Moreover, the differences reported in the last paragraph of Section 3, are also decreased by 1.4%.

Figure 4 shows the normalized solar spectrum at one nanometer resolution. An extension above 2400 nm is possible using the spectrum of Kurucz and Bell (1995) and the scaling coefficient at 2400 nm.

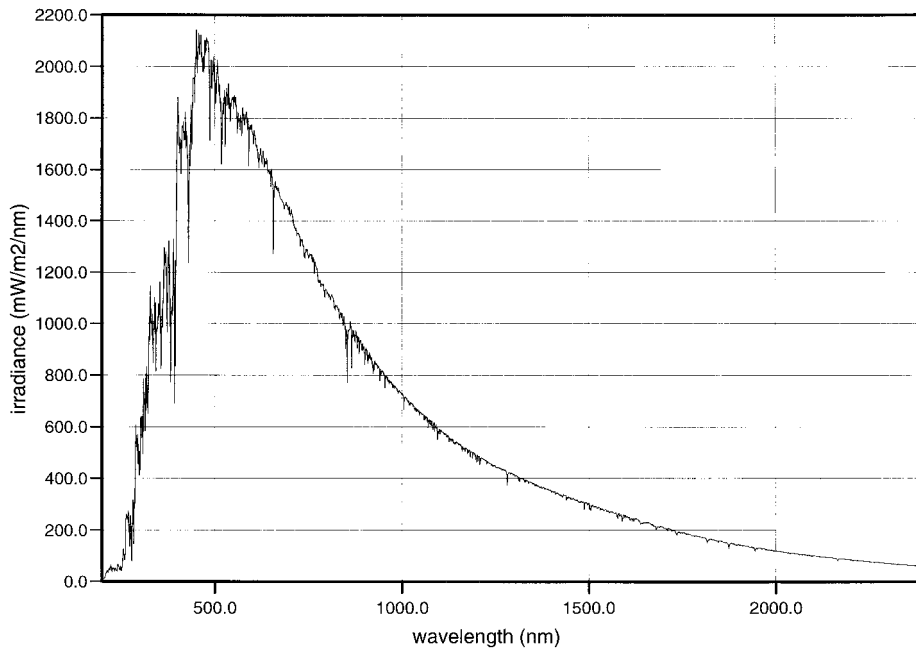


Figure 4. Absolute solar spectral irradiance from the SOLSPEC and SOSIP spectrometers from 200 to 2400 nm after normalization by 1.4%.

No variability in the visible and IR domains was detected by the SOLSPEC and SOSIP instruments. However, the spectrum shown in Figure 4 corresponds for its UV part to the condition of solar activity as observed during the ATLAS 1 mission ($F_{10.7} = 192.4$ units and a monthly mean of 171 units), that is to say, at moderately high solar activity.

5. Conclusion

The SOLSPEC instrument has measured the solar spectral irradiance from 200 to 850 nm at 1 nm resolution during the ATLAS missions. The instrument was calibrated on the PTB standard by use of the Heidelberg Observatory blackbody run at 2930 K. The absolute accuracy, based on a detailed analysis of the sources of uncertainties, indicates a mean absolute uncertainty of 2 to 3%. This analysis shows that the largest sources of uncertainties are the pyrometer calibration, the weakness of the signal during calibration measurements at both ends of the spectral range and after filter changes during the spectral scanning. Detailed comparisons with the SSBUV and SUSIM spectrometers on board ATLAS and with the SOLSTICE and SUSIM on board UARS, show at 5 nm resolution RMS and mean differences of 2 to 3% except at some specific wavelengths. For the visible domain, the best agreement is found with the spectra of Burlov-Vasiljev, Gurtovenko, and Matve-

jev (1995) and Neckel and Labs (1984) above 450 nm while below 450 nm, a difference reaching 6% is found with the latter.

SOSP, the twin instrument of SOLSPEC, flew on board EURECA. It has been also calibrated with the Heidelberg blackbody. The accuracy of the IR measurements is quoted to be about 2%. Above 850 nm, the SOSP/EURECA measurements are compared with solar models and other observations. The latter still contain some telluric signatures. Solar models present a spectral irradiance a few percent smaller than our observations especially above 1800 nm. However, the recent solar model of Fox, Fontenla, and White (2002) is in very close agreement with our observations.

Using the ATLAS 1 and EURECA data, a spectrum covering 200 to 2400 nm is built. The Fraunhofer lines from Kurucz and Bell (1995) are installed at 1 nm resolution. After integration and taking the complement above 2400 nm either from the spectra of Labs and Neckel (1968) or Kurucz and Bell (1995), a comparison with the TSI given by Fröhlich and Lean (1998) shows a 1.4% difference which is within our measurements uncertainties. This percentage has been used to normalize our results. It is mainly originating from the pyrometer calibration, and not from the PTB scale. The resulting spectrum is available by electronic mail.

Acknowledgements

This investigation was supported by the Centre National d'Etudes Spatiales (France), the Centre National de la Recherche Scientifique (France), the Federal Office for Scientific, Technical and Cultural Affairs (Belgium), and the Bundesministerium für Forschung und Technologie (Germany). The participating institutes are the Service d'Aéronomie du CNRS (SA), the Institut d'Aéronomie Spatiale de Belgique and the Landessternwarte of Heidelberg, which provided us with the blackbody for the instrument calibration. The Project Manager of the SOLSPEC and SOSP instruments was T. Foujols (SA) and the data processing was carried out by G. Azria (SA). The ATLAS missions were conducted by NASA and the flight operations were under the Marshall Space Flight Center responsibility. The ESA mission EURECA has been launched and retrieved by the Space Shuttle and the flight operations were conducted by the European Space Operation Center (Darmstadt, Germany). We thank the referee for his pertinent remarks and suggestions.

References

- Arvesen, J. C., Griffin, R. N., Jr., and Pearson, B. D., Jr.: 1969, *Appl. Optics* **8**, 2215.
Avrett, E. H.: 1998, in J. M. Pap, C. Fröhlich, and R. K. Ulrich (eds.), *Proceedings of the SOLERS22 Workshop* held at the National Solar Observatory, Sacramento Peak, Sunspot, New Mexico, June 17–21, 1996, Kluwer Academic Publishers, Dordrecht, Holland, pp. 449–469.

- Brueckner, G. E., Eldow, K. L., Floyd, L. E., Lean, J. L., and VanHoosier, M. E. J.: 1993, *J. Geophys. Res.* **98**, 10695.
- Burlov-Vasiljev, K. A., Gurtovenko, E. A., and Matvejev, Y. B.: 1995, *Solar Phys.* **157**, 51.
- Cebula, R. P., Huang, L. K., and Hilsenrath, E.: 1998, *Metrologia* **35**, 677.
- Cebula, R. P., Thuillier, G., Vanhoosier, M. E. J., Hilsenrath, E., Hersé, M., and Simon, P. C.: 1996, *Geophys. Res. Lett.* **23**, 2289.
- Colina, L., Bohlin, R. C., and Castelli, F.: 1996, *Astrophys. J.* **112**, 307.
- Crommelynck, D., Domingo, V., Fichot, A., Fröhlich, C., Penelle, B., Romero, J., and Werhli, Ch.: 1993, *Metrologia* **30**, 375.
- Crommelynck, D., Fichot, A., Domingo, V., and Lee, R., III: 1996, *Geophys. Res. Lett.* **23**, 2293.
- DeLand, M. T. and Cebula, R. P.: 1998, *J. Geophys. Res.* **103**, 16251.
- Floyd, L. E., Prinz, D. K., Crane, P. C., and Herring, L. C.: 2002, *Adv. Space Res.* **29**, 1957.
- Fontenla, J. M., White, O. R., Fox, P. A., Avrett, E. H., and Kurucz, R. L.: 1999, *Astrophys. J.* **518**, 480.
- Fox, P. A.: 2003, in J. Pap, P. Fox, C. Fröhlich, H. S. Hudson, J. Kuhn, J. McCormack, G. North, W. Sprigg, and S. T. Wu (eds.), *Solar Variability and its Effect on the Earth's Atmosphere and Climate System*, AGU Monograph Series, American Geophysical Union, Washington D.C., in press.
- Fox, P. A., Fontenla, J. M., and White, O. R.: 2002, *Adv. Space Res.*, submitted.
- Fröhlich, C. and Lean, J.: 1998, *Geophys. Res. Lett.* **25**, 4377.
- Gingerich, O. and de Jager, C.: 1968, *Solar Phys.* **3**, 5.
- Holweger, H.: 1967, *Z. Astrophys.* **65**, 365.
- Kurucz, R. L.: 1993, Smithsonian Astrophys. Obs. CD rom # 19.
- Kurucz, R. L. and Bell, B.: 1995, Cambridge, Smithsonian Astrophys. Obs., CD-rom No. 23.
- Labs, D. and Neckel, H.: 1962, *Z. Astrophys.* **55**, 269.
- Labs, D. and Neckel, H.: 1968, *Z. Astrophys.* **69**, 1.
- Livingston, W.: 1992, in R. F. Donnelly (ed.), *Proceedings of the Workshop on Solar Electromagnetic Radiation Study for Solar Cycle 22*, NOAA ERL, Boulder, CO, p. 11.
- Livingston, W. and Wallace, L.: 1991, NSO Technical report # 91-001, NSO, Nat. Opt. Astron. Obs., Tucson.
- Mandel, H., Labs, D., Thuillier, G., Hersé, M., Simon, P. C., and Gillotay, D.: 1998, *Metrologia* **35**, 697.
- Neckel, H. and Labs, D.: 1984, *Solar Phys.* **90**, 205.
- Rottman, G. J., Woods, T. N., and Sparn, T. P.: 1993, *J. Geophys. Res.* **98**, 10667.
- Thekaekara, M. P.: 1974, *Appl. Optics* **13**, 518.
- Thuillier, G., Hersé, M., Simon, P. C., Labs, D., Mandel, H., and Gillotay, D.: 1997, *Solar Phys.* **171**, 283 (Paper 1).
- Thuillier, G., Hersé, M., Simon, P. C., Labs, D., Mandel, H., and Gillotay, D.: 1998a, *Solar Phys.* **177**, 41 (Paper 2).
- Thuillier, G., Hersé, M., Simon, P. C., Labs, D., Mandel, H., and Gillotay, D.: 1998b, *Metrologia* **35**, 697 (Paper 3).
- VanHoosier, M. E. J.: 1996, *SPIE Proceedings* **2831**, 57.
- Wehrli, C.: 1985, *Extraterrestrial Solar Spectrum*, PMOD publication 615.
- Woods, T. N., Prinz, D. K., Rottman, G. J., London, J., Crane, P. C., Cebula, R. P., Hilsenrath, E., Brueckner, G. E., Andrews, M. D., White, O. R., VanHoosier, M. E., Floyd, L. E., Herring, L. C., Knapp, B. G., Pankratz, C. K., and Reiser, P. A.: 1996, *J. Geophys. Res.* **101**, 9541.
- Woods, T. N., Rottman, G. J., Bayley, S. M., Solomon, S. C., and Worden, J.: 1998, *Solar Phys.* **177**, 133.